Journal of
Materials Chemistry B

PAPER

View Article Online
View Journal | View Issue

Cite this: J. Mater. Chem. B, 2015, 3, 6368

Development of a hybrid gelatin hydrogel platform for tissue engineering and protein delivery applications†

Xiaodi Sun,‡[ab] Xin Zhao,‡*[c] Lili Zhao,[d] Qing Li,[ab] Mathew D'Ortenzio,[e] Brandon Nguyen,[e] Xin Xu*[ab] and Yong Wen*[ab]

Received 9th April 2015,
Accepted 3rd July 2015

DOI: 10.1039/c5tb00645g

www.rsc.org/MaterialsB

In this study, to improve the cellular interaction and protein release of gelatin hydrogels, we reported the development of a new hybrid hydrogel platform as a promising tissue engineering scaffold and drug delivery carrier. The biodegradable, biocompatible hybrid hydrogel platform was fabricated from gelatin methacrylamide (Gel-MA) and arginine based unsaturated non-peptide polycations (Arg-UPEA) through UV photo-crosslinking, combining the favorable properties of gelatin and arginine. The hydrogels were systematically characterized based on their mechanical properties, swelling mechanics, interior morphology, and biodegradation capability. The *in vitro* biocompatibility study showed that the hybrid hydrogels show better performance than GelMA hydrogels, in terms of cell attachment and proliferation. Therapeutic proteins were loaded into the hydrogels and their release behavior was investigated. The loading and release profiles indicated that the new cationic gelatin hydrogels could significantly improve the protein loading capabilities, and release the proteins *in vitro* in a sustained manner. The structure-function study indicated that the material composition has a large effect on the properties of the hydrogels.

Introduction

With the ability to swell and hold large amounts of water in the wet state,[1–3] hydrogels generally consist of three-dimensional (3D) material networks that are cross-linked chemically and/or physically.[4,5] Due to their significant water content, hydrogels also possess a degree of flexibility and softness similar to natural tissues.[1–3] Different from other formulations,[6–12] hydrogels have shown significant advantages and attracted strong interest in the fields of tissue engineering and drug delivery because of their high water content, 3D microporous structure, biocompatibility, organic solvent free environment, permeability for oxygen and nutrients, and tissue-like elastic properties.[1–5,12–17]

Among the reported hydrogel systems, natural material based hydrogels, such as dextran, chitosan, hyaluronic acid, alginate and collagen/gelatin, have received plenty of attention due to their high biocompatibility and natural abundance.[18–26] Gelatin, the denatured form of collagen, has been widely utilized and considered as the one of the gold standards in terms of biocompatibility and assisting cell attachment and proliferation.[27–30] Because gelatin itself will dissolve below 37 °C, solid gelatin scaffolds need to be fabricated *via* physical or chemical means.[27–31] The glutaraldehyde crosslinking method is the main chemical strategy,[29,30] however, it may cause the toxicity of the material. For photochemical applications, the gelatin need to be first modified into photo-crosslinkable materials, such as gelatin methacrylamide (Gel-MA).[27,28] However, due to the extremely complicated mechanism of tissue or organ regeneration, the currently available hydrogel scaffolds may not meet the high requirements or demands of tissue engineering under many circumstances.[27,28,32] For example, one of the major limitations is the unsatisfactory cellular attachment and proliferation performance of scaffolds, even for the gelatin based platforms.[27,28,32] The inadequate cellular interactions greatly limit biomedical applications since cellular interactions are critical at the start of tissue/organ regeneration. Another limitation is the low efficacy of delivering and releasing large biomacromolecules, such as proteins and nucleic acids, in a spatiotemporal manner. Due to the large interior pore size, hydrophilicity, 3D microporous structure and fast

[a] School of Stomatology, Shandong University, Wenhuaxi Road 44-1, Jinan, 250012, China. E-mail: xinxu@sdu.edu.cn, wenyong@sdu.edu.cn
[b] Shandong Provincial Key Laboratory of Oral Biomedicine, Jinan, 250012, China
[c] Center for Biomedical Engineering, Department of Medicine, Brigham and Women's Hospital, Harvard Medical School, Cambridge, MA, 02139, USA. E-mail: xinzhao02@fas.harvard.edu
[d] Department of Endoscopy, The First Affiliated Hospital of Nanjing Medical University, Jiangsu Province Hospital, Nanjing, Jiangsu, 210029, China
[e] University of Waterloo, 200 University Avenue West, Waterloo, ON N2L 3G1, Canada

† Electronic supplementary information (ESI) available. See DOI: 10.1039/c5tb00645g

‡ Co-first author.

diffusion of drug molecules in aqueous environments, hydrogel releasing rates of drugs are normally rapid.[14] Other key limitations include unacceptable and uncontrollable biodegradation rates and mechanical properties.[27,28,32] Here one important question arises: without decreasing their biocompatibility, could the gold standard hydrogel platforms show enhanced cellular interactions and drug release performance, along with tuneable mechanical properties/biodegradation rates?

For the above question, a few strategies have been investigated for plenty of hydrogel platforms, including physically mixing new components/systems and chemical modifications.[33–36] Among them, fabricating hybrid hydrogels containing two or more components (precursors) have aroused strong interests.[26,37–39] The chemical introduction of new functional precursors could help to tune or bring new properties/functionalities to hydrogels, these may include charge properties, mechanical properties, tuneable degradation rates, hydrophobic/hydrophilic properties, pH and temperature responsive properties, and functional groups.[26,33–39]

In this study, aiming to obtain new gelatin based hydrogel platforms with better biological and drug release performance than the collagen/gelatin hydrogels, we proposed the following hypothesis: the chemical introduction of cationic arginine unsaturated poly(ester amides) into gelatin hydrogels could significantly improve their cellular interactions, tune the degradation rate and mechanical property, while keeping excellent biocompatibility because of their inherent strong cationic property and biocompatibility. Gelatin was chemically modified here into photo-crosslinkable gelatin methacrylamide (Gel-MA). The second components, a family of arginine based unsaturated poly(ester amide)s (Arg-UPEA), were developed due to their strong cationic properties, tunable properties, very low cytotoxicity and muted inflammatory response.[37] The hydrogels were fabricated by UV photo-crosslinking, from the mixture of Gel-MA and Arg-UPEA aqueous solutions. The physicochemical properties, biocompatibility and biological performance of the hydrogels were then systematically evaluated. In addition, to evaluate the capability for sustainable release of proteins, bone morphogenetic protein (BMP) was selected as a model protein drug in this study, and was pre-loaded into the hydrogels before photo-crosslinking. The various hydrogel formulations were then characterized in terms of *in vitro* release kinetics.

Experimental

Materials

Type A porcine skin gelatin (gel strength 300, cat No: G2500, M_W around 330 kD), 2-hydroxy-*l*-[4-(hydroxyethoxy)phenyl]-2-methyl-l-propanone (Irgacure 2959), L-Arginine (L-Arg), *p*-toluenesulfonic acid monohydrate, fumaryl chloride, ethylene glycol, 1,4-butanediol, 1,6-hexanediol, *p*-nitrophenol, triethylamine and lipopolysaccharide (LPS, from *E. coli* 0111:B4) were purchased from Sigma-Aldrich (St. Louis, MO) and used without further purification. BMP-2 and BMP-2 ELISA kits were purchased from R&D systems. The TNF-α ELISA kit was purchased from Invitrogen (Carlsbad, CA). Other chemicals and reagents, if not otherwise specified, were purchased from Sigma-Aldrich (St. Louis, MO).

Synthesis of hydrogel precursors

The Gel-MA precursor was synthesized following a previously reported method.[27,28] Briefly, 6.0 mL of methacrylic anhydride was added into 100 mL of 10 wt% gelatin phosphate buffer solutions (PBS) at 60 °C, and was vigorously stirred for 3 h. After purification, Gel-MA was obtained with a degree of methacrylation of around 50–60%. The Arg-UPEAs were synthesized by the polycondensation method reported before.[37,40] Briefly, the unsaturated di-*p*-nitrophenyl ester of dicarboxylic acid (**I**) and tetra-*p*-toluenesulfonic acid salts of bis(L-arginine), α,ω-alkylene diesters (**II**) were prepared first following previous reports. After that, the Arg-UPEA (**III**) was prepared *via* solution polycondensation of (**I**) and (**II**). The molecular weight (M_W) of Arg-UPEA is around 10.0–15.0 kg mol^{-1}. The Gel-MA or Arg-UPEA precursors were purified first by dissolving the precursors in distilled water and were dialyzed against deionized water (M_W cut off 4000) under a dark environment for 5 days. Next, the solutions were lyophilized for 5 days using a freeze-drier at −45 °C.

Preparation of hydrogels

Gel-MA/Arg-UPEA hybrid hydrogels were prepared by the photopolymerization of two precursors (Gel-MA and Arg-UPEA) at different weight ratios in aqueous solution with an initiator. An example of the fabrication protocol is given below: 0.40 g of Gel-MA, 0.10 g of 2-UArg-2-S and 5.0 mg of photoinitiator Irgacure 2959 (1.0 wt% of total amount of precursors) were added into a glass vial and dissolved in 3.5 mL of distilled water to form a clear homogeneous solution. The solution mixture was then transferred into a 20-well Teflon mold (diameter 12 mm and thickness ≈ 4 mm for each well). Then, the precursor solution in the mold was irradiated using a long-wavelength UV lamp (365 nm, 100 W) for a specific time (normally 1–2 min) at room temperature. The irradiation distance was 5–10 cm. After fabrication, the resultant hydrogels were removed from the mold and soaked for 24 h in distilled water or buffer to remove the toxic residues, then dried in a vacuum at room temperature for 24 h prior to further characterization. For protein loaded hydrogels, a pre-determined amount of proteins was mixed with the precursor solution before photo-crosslinking. All other fabrication conditions were same.

Equilibrium swelling ratio and swelling kinetics of hydrogels

The equilibrium swelling ratio (Q_{eq}) of the hydrogel is calculated by the following equation: $Q_{eq} = [(W_e - W_d)/W_d] \times 100\%$, where W_e is the weight of a swollen hydrogel at equilibrium, and W_d is the weight of the corresponding dry hydrogel at $t = 0$. All swelling ratio results were obtained from triplicate samples and data were expressed as the mean ± standard deviation. The swelling kinetics of the Gel-MA/Arg-UPEA hydrogels was measured over a period of 48 h at room temperature. Each dry Gel-MA/Arg-UPEA hydrogel sample was weighed and immersed in 20 mL of solutions with different parameters for predetermined periods. Before weighing, the samples were taken from

the solutions and blotted with filter papers to remove excess surface water. The swelling ratio (Q) of the hydrogels, at time t, is calculated using the following equation: $Q = [(W_t - W_d)/W_d] \times 100\%$.

Compressive modulus of hydrogels

The mechanical properties of the Gel-MA/Arg-UPEA hydrogels were measured using a 2980 Dynamic Mechanical Analyzer (DMA) (TA Instruments Inc., New Castle, DE) in "controlled force" (CF-mode) mode. The swollen hydrogel samples, as circular discs, were submerged in distilled water and mounted between the movable compression clamp (diameter 30 mm) and the fluid cup with a 0.1 N preloading force. A force ramp from 0.1 N at a rate of 0.3 or 0.5 N min^{-1} was applied. All measurements were carried out at room temperature. The compression elastic modulus (E) of the swollen hydrogel was extracted by plotting the compressive stress *versus* strain. All compression elastic modulus data in this study were obtained from triplicate samples and data were expressed as mean ± standard deviation.

In vitro enzymatic biodegradation of hydrogels

The *in vitro* biodegradation of the Gel-MA/Arg-UPEA hybrid hydrogels was evaluated using collagenase type II.[41] Briefly, a freshly prepared and purified hydrogel was placed in a glass vial containing 10 mL of PBS buffer (pH 7.4, 0.067 M) or 2 U mL^{-1} collagenase in 10.0 mL of PBS buffer. The hydrogel (dry weight around 0.10–0.20 g) was then incubated at 37 °C with constant reciprocal shaking (*ca.* 100 rpm). At the end of a predetermined period, the hydrogels were removed (or collected by filtration if broken into small parts), then washed with distilled water 3 times, and dried in a freeze drying machine for 24 h to completely remove the residue water. The collagenase solution was refreshed every other day to maintain enzyme activity.

Interior morphology of hydrogels

Interior morphology of Gel-MA/Arg-UPEA hydrogels was investigated using a scanning electron microscope (SEM). The swollen hydrogel samples, after reaching their maximum swelling ratio in distilled water at room temperature, were quickly frozen in liquid nitrogen and then freeze-dried under vacuum at −48 °C for 2 days until all water inside the hydrogel was sublimed. The freeze-dried hydrogel samples were then cut, fixed on aluminum stubs, and coated with gold for 30 seconds for interior morphology observation with a SEM instrument (Leica S440, Germany).

Cell attachment and proliferation on the hydrogel surface and inside the hydrogel

The cellular interaction of the Gel-MA/Arg-UPEA hybrid hydrogel surface and inside hydrogel was evaluated in terms of the cell attachment and proliferation performance. For cellular interaction on hydrogel surface, pure Gel-MA and PEG-DA (M_W 8000) hydrogels were selected as the hydrogel controls. The cells used for this study were HeLa cells (ATCC, Manassas, VA). The purified swollen hydrogels were cut into round shapes with a diameter that just filled the well of a 24-well cell culture plate, and incubated at 37 °C in cell culture media. The hydrogels were sterilized under UV light (in the cell culture hood) for at least 2 h before being put into the 24-well cell culture plates. After that, the hydrogels were washed twice by PBS buffer and cell culture media. Then, the hydrogels were placed in the wells of the cell culture plate and fixed by a sterilized rubber ring, which had the same diameter as the well of cell culture plate. The cells were seeded at an appropriate cell density (40 000 cells per well) and incubated overnight. The media was changed after 12 h to wash the unattached cells. After 48 h of incubation, the cell attachment and proliferation on the hydrogel surface was recorded using an optical microscope. For cellular interaction study inside hydrogels, precursors/initiators were pre-dissolved in serum free medium (5.0 wt%). Then the solution was quickly mixed with predetermined amount of freshly collected NIH 3T3 fibroblasts (cell concentration 1 million per mL gel). The mixed solution was then transferred into 96 well cell culture plates (100 μL per well), irradiated using the 100 W UV lamp for 1 min at room temperature. After that, 100 μL 20 wt% FBS media was added into each well and the cells encapsulated in hydrogels were cultured at 37 °C in 5% CO_2. Medium was replaced everyday. Cell proliferation was enumerated using PicoGreen®DNA quantification assay. 500 μL of 50 μg mL^{-1} proteinase K solution was added to each sample followed by incubation at 37 °C overnight and subsequent centrifugation at 4 °C at 14 000 rpm for 10 min. In the dark, 100 μL of supernatant was mixed with 100 μL of PicoGreen solution (1 : 200 dilution) for 5 min. Using 485 and 520 nm as excitation and emission wavelengths respectively, fluorescence of the samples was measured using a microplate reader (BioTex, Inc. TX).

In vitro inflammatory response of hydrogels

The *in vitro* inflammatory response of the Gel-MA/Arg-UPEA hydrogel was studied according to the reported protocol.[23] J774 macrophages (ATCC, Manassas, VA) were seeded onto the hydrogel surface in 24-well tissue culture plates at a cell concentration of 10 000 cells per well. Positive controls were glass coverslips in media containing LPS at final concentrations of 1.25 μg mL^{-1} and 5.00 μg mL^{-1}. A cell free medium alone was used as a cell-free negative control. Cells cultured without hydrogels and Gel-MA hydrogels were also used as controls. Macrophage activation after 48 h of incubation was measured using an ELISA kit, to measure released mouse TNF-α according to the manufacturer's protocol. Sample TNF-α concentrations were calculated from a standard calibration curve using a 4-parameter standard curve-fitting algorithm (Gen5 software, BioTek Instruments, Winooski, VT). All testing samples were run in triplicate ($N = 3$). All samples and standards were read in duplicate on a 96-well plate reader at 450 nm and referenced against a chromogen blank.

Controlled release of proteins *via* hydrogels

The release of BMP-2 from the Gel-MA/Arg-UPEA hydrogels was carried out in a PBS buffer solution at 37 °C. Proteins were preloaded into the hydrogel samples according to the following protocol: pre-determined amounts of protein were directly mixed with Gel-MA first, then mixed with Arg-UPEA precursors

and photo-initiators in distilled water, and finally the solution mixture was UV irradiated for 1–2 min to form protein loaded hydrogels. The protein loaded hydrogels were then placed inside small vials containing 10.0 mL PBS solution (one piece of hydrogel per vial). The vial was incubated at 37 °C with constant reciprocal shaking (*ca.* 100 rmp). The protein contents were then analyzed by an ELISA assay. The released BMP-2 proteins were also collected and compared with the untreated BMP-2 proteins (same concentration) using ELISA assay. All protein release tests, at each time point, were carried out in triplicate and the variation was expressed as a standard error of the mean.

Results and discussion

It has been reported that arginine-based material could improve the cellular interactions of synthetic and natural hydrogels. However, these improvements are based on the poor or normal cellular performance of the original hydrogels. For those "gold standard" hydrogels with superior cellular interaction performance, whether Arg-UPEA could help the improvements has not yet been investigated. To achieve excellent cellular interactions, especially for the gelatin based hydrogel platforms, we developed a novel biocompatible and biodegradable hybrid hydrogel platform utilizing a new simple fabrication strategy. This would maximally keep the original properties of hydrogels and be suitable for tissue engineering and drug delivery applications. Subsequently, the hybrid hydrogel system combines the favorable properties of Gel-MA and arginine polymer (high pK_a). The variety of the hydrogel component types and parameters (molecular weight, component ratio, crosslinking density) can allow us to engineer the hydrogel platforms for a wide range of tissue engineering and drug delivery needs.

Synthesis of precursors

In this report, Gel-MA was chosen as a precursor component due to its excellent biocompatibility, water solubility, low toxicity, low immunogenicity and photocrosslinkability. The synthesis and characterization details of the Gel-MA could be found in the ESI.†

For Arg-UPEAs, the synthesis and characterization details can also be found in the ESI.† The unsaturated di-*p*-nitrophenyl ester of dicarboxylic acid (Monomer **I**, di-*p*-nitrophenyl fumarate (NF), $x = 2$) was prepared by reacting fumaryl chloride with *p*-nitrophenol as previously reported. Moreover, three types of *p*-toluenesulfonic acid salt of L-arginine diesters (Monomer **II**) were prepared in this study: tetra-*p*-toluenesulfonic acid salt of bis(L-arginine)ethane diesters Arg-**2**-S ($y = 2$); tetra-*p*-toluenesulfonic acid salt of bis(L-arginine)butane diesters, Arg-**4**-S ($y = 4$); tetra-*p*-toluenesulfonic acid salt of bis(L-arginine)hexane diesters, Arg-**6**-S ($y = 6$). Arg-UPEAs were prepared by the solution polycondensation of (**I**) and (**II**) monomers at different combinations. The Arg-UPEAs synthesized here with different combinations of diacids and diols building blocks were: 2-UArg-2-S, 2-UArg-4-S and 2-UArg-6-S. The three Arg-UPEAs synthesized have significantly different solubility in aqueous solutions due to the different CH_2 segment in the repeating unit, indicating different hydrophobicity.

Fabrication of hydrogels

In this report, Gel-MA and Arg-UPEA were photo-crosslinked by UV treatment, with Irgacure 2959 as the photo initiator in an aqueous system. For easy comparison, the amount of Gel-MA in solution was fixed at 10 wt%. To keep the gelatin as the majority component of hydrogel, the weight ratio of Gel-MA to Arg-UPEA was chosen at 9 : 1, 4 : 1, or 3 : 2 in this report. In this study, the hybrid hydrogel was named: Gel-MA/Arg-UPEA (m/n, w/w), where m/n is the weight ratio of Gel-MA to Arg-UPEA. Table S1 (ESI†) is the summary of the developed hydrogels. The photo-crosslinking time was suggested to be as short as possible so that the bioactivity of the proteins would not be affected. Meanwhile, to maximally reduce the side crosslinking of Gel-MA and Arg-UPEA, the precursor should be completely mixed well and the crosslinking rate should also be as quick as possible. Therefore, a 100 W UV light is utilized so that the photo-crosslinking could be finished within minutes (typically 1–2) depending on the composition of the hydrogel. An increased amount of Arg-UPEA inside the hydrogel would need a longer time due to the relative weak reactivity of the double bonds of Arg-UPEA. Fig. 1 showed the chemical structure of Gel-MA, Arg-UPEA and the image of a Gel-MA/2-UArg-2-S hydrogel (swollen (left) and dry (right)). All the fabricated GEL-MA/Arg-UPEA hydrogels in this report were light white or colorless after reaching their swelling equilibrium. The yields of formed hydrogels were evaluated in terms of the mass conversion percentage. Table S1 (ESI†) indicates that the percentage is high (around or above 90 wt%), which may be due to the very high UV irradiation power, causing the crosslinking to be finished within seconds or minutes. The successful formation of hydrogels was confirmed by the formation of stable 3D scaffolds and the other characteristics including swelling capability, mechanical properties, interior 3D morphology (SEM), enzyme biodegradation and other properties.

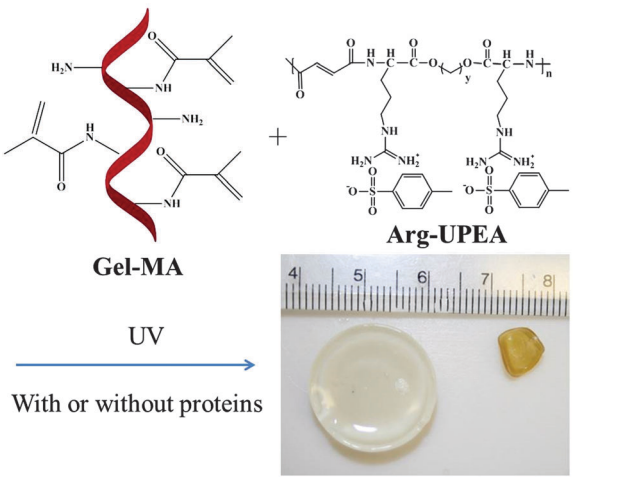

Fig. 1 Illustration of the chemical structure of hydrogel precursors (Gel-MA (left) and Arg-UPEA (right)) and the photo image of Gel-MA/2-UArg-2-S (4 : 1, w : w) hydrogel (swollen (left) and dry (right)).

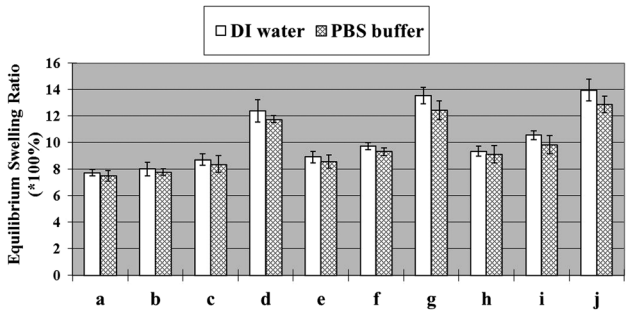

Fig. 2 Equilibrated swelling ratio of Gel-MA/Arg-UPEA hydrogels in PBS (pH = 7.4) solution and DI water at room temperature. (a) Gel-MA; (b) Gel-MA/2-UArg-2-S (9/1, w/w); (c) Gel-MA/2-UArg-2-S (4/1, w/w); (d) Gel-MA/2-UArg-2-S (3/2, w/w); (e) Gel-MA/2-UArg-4-S (9/1, w/w); (f) Gel-MA/2-UArg-4-S (4/1, w/w); (g) Gel-MA/2-UArg-4-S (3/2, w/w); (h) Gel-MA/2-UArg-6-S (9/1, w/w); (i) Gel-MA/2-UArg-6-S (4/1, w/w); (j) Gel-MA/2-UArg-6-S (3/2, w/w).

Equilibrated swelling ratio and swelling kinetics of hydrogels

The swelling activity of the developed hydrogels was systematically investigated in terms of the equilibrated swelling ratio and the swelling kinetics as a function of hydrogel compositions (the weight feed ratio of Gel-MA to Arg-UPEA) and y value of Arg-UPEA.

For the swelling ratios at equilibrium (SRE), they were tested in both 1X PBS buffer solutions and deionized water (DI water). Fig. 2 shows the SRE at room temperature for the Gel-MA hydrogels. Due to the strong cationic property of Arg-UPEA, the SRE of Gel-MA/Arg-UPEA hydrogels in DI water was always slightly higher than that of the corresponding hydrogels in PBS solution. Additionally, the SRE of all Gel-MA/Arg-UPEA hybrid hydrogels were higher than that of pure Gel-MA hydrogel both in DI water and PBS, respectively. These results implied that the introduction of Arg-UPEA moiety did enhance the SRE of the hybrid hydrogels. The SRE of the hybrid hydrogels generally increase with the increasing of weight feed ratio of Arg-UPEA to Gel-MA either in PBS buffer or DI water. Furthermore, the SRE of the hybrid hydrogels increase with an increase of the y value of the Arg-UPEA either in DI water or PBS solution at a fixed weight ratio of Arg-UPEA to Gel-MA.

The swelling kinetics of the Gel-MA/Arg-UPEA hydrogel was studied over a period of 3 days in deionized (DI) water at room temperature. Fig. 3 shows that the hydrogels with various compositions (different types of Arg-UPEAs or feed weight ratio of Gel-MA to Arg-UPEA) had a high swelling rate during the initial 2 h. After the initial 2 h, the swelling rate leveled off, and finally reached their swelling equilibrium within 14–18 h. Compared with the pure Gel-MA hydrogel, the corresponding Gel-MA/Arg-UPEA hydrogel did not show an obvious swelling rate difference.

Compressive modulus of hydrogels

Fig. 4 shows a comparison of the mechanical properties of the swollen Gel-MA/Arg-UPEA hydrogels in terms of the compression elastic modulus. Compared with Gel-MA (control), a small amount of Arg-UPEA may slightly increase the compression modulus. After chemically introducing more Arg-UPEA into the

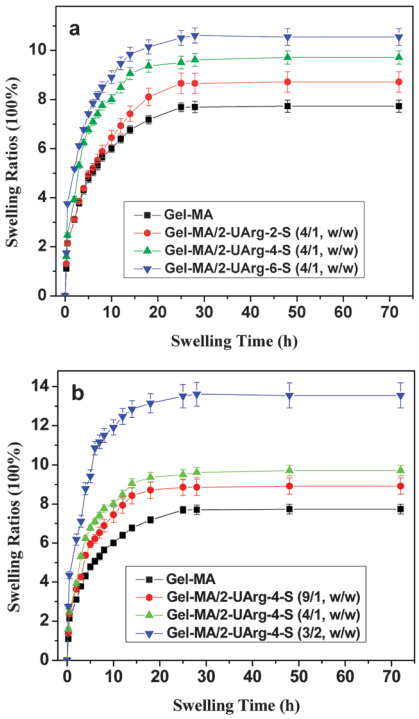

Fig. 3 Swelling kinetics of the Gel-MA/Arg-UPEA hydrogel in DI water at room temperature: (a) effect of Arg-UPEA types; (b) effect of Arg-UPEA weight percentage.

Gel-MA hydrogel, the modulus decreases, but within the same magnitude. In this platform, the types of Arg-UPEA may not show significant difference.

Interior morphology (SEM) of Arg-UPEA/hydrogels

The cross-sectional interior morphology of the freeze-dried GEL-MA/Arg-UPEA hydrogel was examined by SEM to understand the 3D structure of hybrid hydrogel. Even though the interior structure/morphology of hydrogel after freeze-drying would be different from the natural state of the swelling hydrogel, it is still helpful for understanding the detail of the hydrogel 3D interior micro-structure. As shown in Fig. 5, compared with Gel-MA hydrogels, the GEL-MA/Arg-UPEA hydrogel has a similar average pore size (5–10 μm) and cell wall thickness, but with a slight

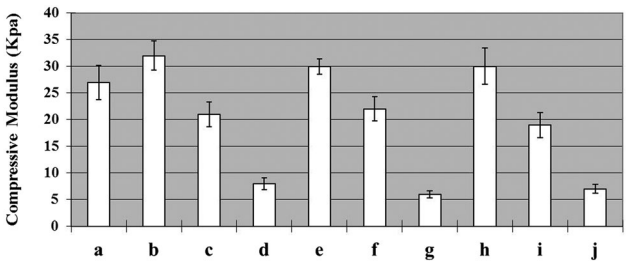

Fig. 4 Compressive modulus of swollen hydrogels: (a) Gel-MA; (b) Gel-MA/2-UArg-2-S (9/1, w/w); (c) Gel-MA/2-UArg-2-S (4/1, w/w); (d) Gel-MA/2-UArg-2-S (3/2, w/w); (e) Gel-MA/2-UArg-4-S (9/1, w/w); (f) Gel-MA/2-UArg-4-S (4/1, w/w); (g) Gel-MA/2-UArg-4-S (3/2, w/w); (h) Gel-MA/2-UArg-6-S (9/1, w/w); (i) Gel-MA/2-UArg-6-S (4/1, w/w); (j) Gel-MA/2-UArg-6-S (3/2, w/w).

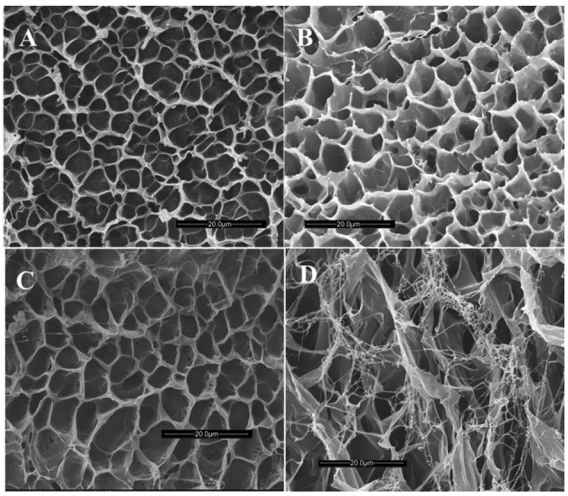

Fig. 5 SEM images of freeze dried Gel-MA and Gel-MA/2-UArg-2-S hybrid hydrogel (A: Gel-MA; B: Gel-MA/2-UArg-2-S (9/1, w/w); C: Gel-MA/2-UArg-2-S (4/1, w/w); D: Gel-MA/2-UArg-2-S (3/2, w/w)). Scale bar is 20 μm.

higher number of nanofibers entangled with the hydrogel cells. 10 wt% or 20 wt% of Arg-UPEA may not bring many nanofibers, but 40 wt% of Arg-UPEA does cause obvious fibrous nanostructures. These fibrous nanostructures may be helpful to assist the formation of vascular structures or improve the sustained release of proteins.

Biodegradation of hydrogels

Fig. 6 shows the biodegradation results of Gel-MA/Arg-UPEA hydrogels. Before biodegradation, all the hydrogels were soaked in buffers for 24 h to remove the residues. In PBS buffer, without collagenase type II enzyme, all the hydrogels showed a slow degradation within 5 weeks. The types of Arg-UPEA did not show obvious changes. However, the addition of 2 U mL^{-1} of collagenase enzyme helps to degrade the pure Gel-MA hydrogel completely within two weeks. The 2 U mL^{-1} collagenase concentration was around the concentration found during wound healing.[42] For the effects of Arg-UPEA types, the results indicated that Gel-MA/Arg-UPEA (1 : 4, w/w) hydrogels showed relative slower degradation than the Gel-MA. This indicates that the introduction of Arg-UPEA would cause a relatively slower degradation, possibly due to the charge interaction with enzymes and the more complicated 3D structure. The degradation curves for enzyme treated groups ended before 100 wt% because the degraded hydrogel debris were difficult to collect.

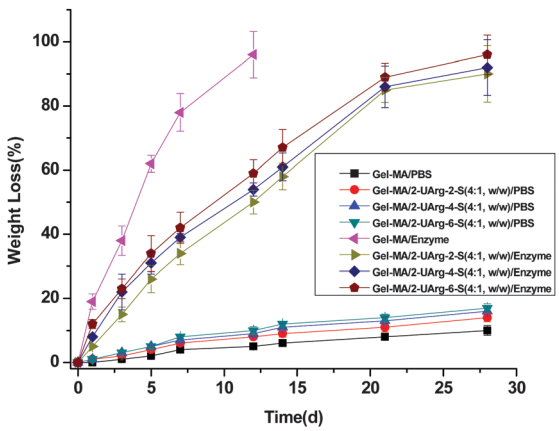

Fig. 6 Biodegradation of the Gel-MA/Arg-UPEA hydrogels at 37 °C in PBS buffer or enzyme solution.

Cell attachment and proliferation on the hydrogel surface and inside hydrogels

An excellent cellular interaction for the hydrogel is normally considered as a prerequisite for its potential application.[43] Subsequently, one of the main goals of this report is to investigate the possibility to enhance the cellular interaction performance of the Gel-MA hydrogel, a type of collagen-based hydrogel. Here the cellular interaction with Gel-MA/Arg-UPEA hybrid hydrogels was studied in terms of the cell attachment and proliferation on hydrogel surface and inside hydrogels.

For the cellular interaction on surface, the HeLa cells were cultured with a high density on the surface of Arg-UPEA hybrid hydrogels to investigate the cell attachment and proliferation performance. High cell density is used to obtain the cell density difference in terms of the attached cells. After 12 h, the medium was changed and the cells were slightly washed to remove those that are unattached or weakly attached. Fig. 7 showed the example of the HeLa cells cultured for 48 h on the surface of pure the Gel-MA hydrogel, the PEG-DA hydrogel, and the Gel-MA/2-UArg-2-S hybrid hydrogel with different weight ratios, respectively. Compared with the pure PEG-DA hydrogel control (Fig. 7b), the pure Gel-MA hydrogel (Fig. 7a) demonstrated a better cell morphology (fully attached and expanded) and higher amounts of attached/proliferated (high density) HeLa cells after 48 h; which was normal and reasonable for Gel-MA hydrogels. Furthermore, after the introduction of Arg-UPEA, the result (Fig. 7c–e) indicated that the Arg-UPEA did not change the morphology of the attached cells, but significantly enhance the density of attached cells. Fig. 7c–e illustrated the example of the HeLa cells cultured for 48 h on the surface of the Gel-MA/2-UArg-2-S hybrid hydrogel with different weigh ratios. Therefore, the cell culture results indicated that the 2Arg-UPEA could support and enhance the cell attachment and proliferation.

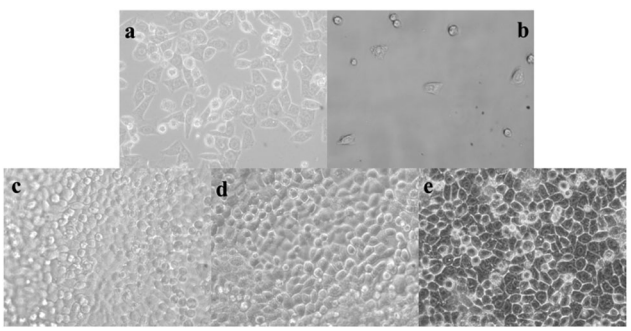

Fig. 7 Representative micrographs of HeLa cells after 48 h culture on the hydrogel surface, 10×. Cells cultured on the hydrogel surface: (a) Gel-MA; (b) PEG-DA; (c) Gel-MA/2-UArg-2-S (9/1, w/w); (d) Gel-MA/2-UArg-2-S (4/1, w/w); (e) Gel-MA/2-UArg-2-S (3/2, w/w).

Furthermore, the normal cells, such fibroblasts, were encapsulated into hydrogels to compare the cellular spreading and proliferation inside the hydrogels. After 1 day, the live-dead assay results (Fig. 8) indicated that the majority of the encapsulated cells were alive (green) for Gel-MA and Gel-MA/2-UArg-2-S (4/1, w/w) groups. The different size and intensity of the light dots confirmed that the cells were in the different sites of the 3D hydrogel scaffolds. Comparing with Gel-MA group, Gel-MA/2-UArg-2-S (4/1, w/w) group exhibited comparable cell survival to the control Gel-MA but improved cell spreading (spreading of cells encapsulated in Gel-MA/2-UArg-2-S could be observed after 1 day culture). After 3 days, the encapsulated cells all spread and proliferated (Fig. 9). Both groups showed high amount of living cells with complete attachment and the Gel-MA/2-UArg-2-S (4/1, w/w) group shows obvious higher degree of cell spreading (compare Fig. 9a and b), possibly due to the positive charges of Gel-MA/2-UArg-2-S, enhancing cell spreading. Moreover, cell proliferation was enhanced when 2-UArg-2-S was incorporated into the Gel-MA hydrogels (Fig. 10) as suggested by the picogreen DNA quantification assay.

All these results indicated that this new hybrid hydrogel platform has great potential to act as a new type of scaffold for tissue engineering and drug delivery applications.

In vitro inflammatory response of hydrogels

In this report, to evaluate the *in vitro* inflammatory response from mouse J774 macrophage activation after being cultured on hydrogel surface for 48 h, an ELISA assay was utilized to measure the TNF-α produced from the macrophage. The *in vitro* inflammatory results (Fig. 11) showed that both Gel-MA and Gel-MA/Arg-UPEA hydrogels exhibited a low level inflammatory response. The increasing amount of Arg-UPEA component percentage did not show an obvious change in terms of TNF-α production. Therefore, the introduction of Arg-UPEA into Gel-MA hydrogel did not increase the inflammation response of Gel-MA. Other hydrogels were not used here for comparison due to the low macrophage attachment on their surfaces.

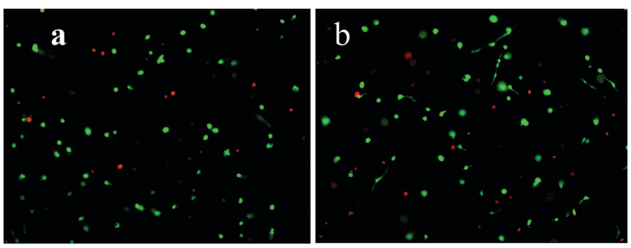

Fig. 8 Viability of NIH 3T3 fibroblasts after 1 day culture inside the hydrogel, 10×. (a) Gel-MA; (b) Gel-MA/2-UArg-2-S (4/1, w/w). Green: living cells; red: dead cells.

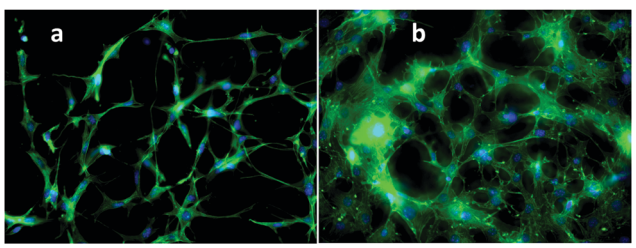

Fig. 9 Representative fluorescent micrographs of NIH 3T3 fibroblasts after 3 day culture inside the hydrogel, 10×. (a) Gel-MA; (b) Gel-MA/2-UArg-2-S (4/1, w/w). Phalloidin stains cell filament green and DAPI stains cell nuclei blue.

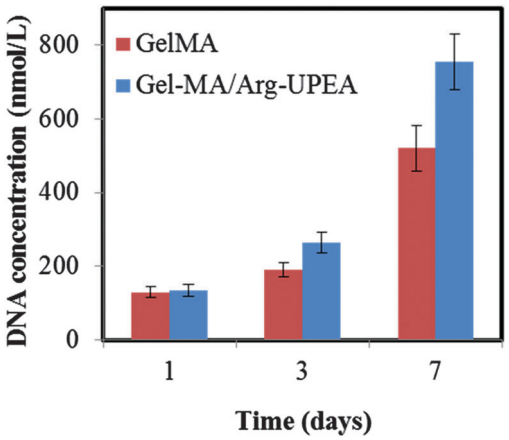

Fig. 10 Proliferation of NIH 3T3 fibroblasts after 7 days culture inside the hydrogels (Gel-MA and Gel-MA/2-UArg-2-S (4/1, w/w)).

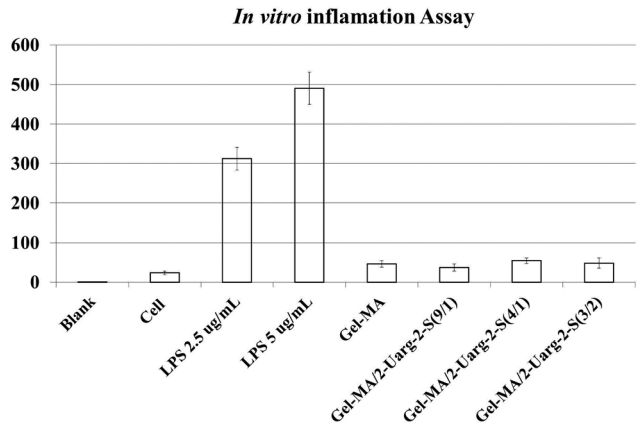

Fig. 11 *In vitro* inflammation assay of hydrogels.

Controlled release of BMP-2 *via* Gel-MA/Arg-UPEA hybrid hydrogels

The sustained release of protein drugs is still a challenge for most of the hydrogel system. With the introduction of a strong cationic moiety, the new platform is expected to be able to release the proteins in a more controllable manner. With a loaded BMP of 5 μg per hydrogel pellet, Fig. 12 demonstrates the protein release profiles from hydrogels in PBS buffer at 37 °C. The BMP content was then analyzed by an ELISA assay. Subsequently, the release data from pure Gel-MA hydrogel showed that the free BMP-2 release was completed around 2–3 days. For the Gel-MA/2-UArg-2-S hydrogel, the protein release was completed around 5–10 days due to the strong electrostatic interaction between Arg-UPEA and BMP-2. An

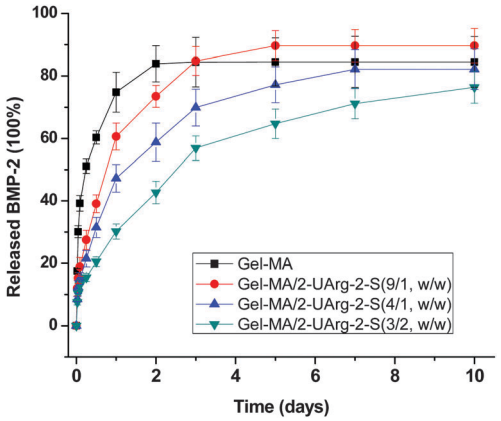

Fig. 12 Controlled release of BMP-2 from hydrogels.

increase of percentage of the Arg-UPEA component would cause slower protein release. The bioactivity comparison (Fig. S10, ESI†) indicated there is no obvious bioactivity change for BMP-2 after being released from the Gel-MA/2-UArg-2-S hydrogel.

Conclusions

A new biocompatible and biodegradable Gel-MA/Arg-UPEA hybrid hydrogel platform was successfully developed *via* UV photo-crosslinking as a promising tissue engineering scaffold and drug delivery carrier. The physicochemical, swelling, mechanical, and morphological properties were systematically investigated. Conclusively, cellular tests indicated that Gel-MA/Arg-UPEA hydrogels show excellent cell attachment and proliferation on its hydrogel surface and inside the hydrogel, better than the Gel-MA itself. A drug release study of BMP-2 also showed that the controlled and sustained release of protein drugs could be achieved for a few days, depending on the hydrogel composition. The excellent biocompatibility and interesting controllable drug release profiles of these hybrid hydrogels reveal that the hybrid cationic hydrogel system developed in this study would have the great potential to act as a tissue engineering scaffold and drug carrier.

Acknowledgements

Project is supported by the National Natural Science Foundation of China (Grant No. 81300885) and Shandong Provincial Natural Science Foundation Grant No: (ZR2013HQ052; ZR2013HM086). Yong Wen is supported by Young Scholars Program of Shandong University (YSPSDU).

Notes and references

1 N. A. Peppas, J. Z. Hilt, A. Khademhosseini and R. Langer, *Adv. Mater.*, 2006, **18**, 1345–1360.
2 K. Y. Lee and S. H. Yuk, *Prog. Polym. Sci.*, 2007, **32**, 669–697.
3 S. Varghese and J. H. Elisseeff, *Adv. Polym. Sci.*, 2006, **203**, 95–144.
4 A. S. Hoffman, *Adv. Drug Delivery Rev.*, 2002, **54**, 3–12.
5 K. Y. Lee and D. J. Mooney, *Chem. Rev.*, 2001, **101**, 1869–1879.
6 N. Bertrand, J. Wu, X. Xu, N. Kamaly and O. C. Farokhzad, *Adv. Drug Delivery Rev.*, 2014, **66**, 2–25.
7 J. Panyam and V. Labhasetwar, *Adv. Drug Delivery Rev.*, 2003, **55**, 329–347.
8 Z. Zhao, J. Wang, H.-Q. Mao and K. W. Leong, *Adv. Drug Delivery Rev.*, 2003, **55**, 483–499.
9 K. W. Leong and R. Langer, *Adv. Drug Delivery Rev.*, 1988, **1**, 199–233.
10 Y. Pan, X. Du, F. Zhao and B. Xu, *Chem. Soc. Rev.*, 2012, **41**, 2912–2942.
11 J. Wu, N. Kamaly, J. Shi, L. Zhao, Z. Xiao, G. Hollett, R. John, S. Ray, X. Xu, X. Zhang, P. W. Kantoff and O. C. Farokhzad, *Angew. Chem., Int. Ed.*, 2014, **53**, 8975–8979.
12 Y. Wen, W. Liu, C. Bagia, S. Zhang, M. Bai, J. M. Janjic, N. Giannoukakis, E. S. Gawalt and W. S. Meng, *Acta Biomater.*, 2014, **10**, 4759–4767.
13 D.-Q. Wu, J. Wu and C.-C. Chu, *Soft Matter*, 2013, **9**, 3965–3975.
14 J. Wu, X. Zhao, D. Wu and C.-C. Chu, *J. Mater. Chem. B*, 2014, **2**, 6660–6668.
15 S. K. Seidlits, C. T. Drinnan, R. R. Petersen, J. B. Shear, L. J. Suggs and C. E. Schmidt, *Acta Biomater.*, 2011, **7**, 2401–2409.
16 D.-Q. Wu, J. Wu, X.-H. Qin and C.-C. Chu, *J. Mater. Chem. B*, 2015, **3**, 2286–2294.
17 Y. Wen, H. R. Kolonich, K. M. Kruszewski, N. Giannoukakis, E. S. Gawalt and W. S. Meng, *Mol. Pharmaceutics*, 2013, **10**, 1035–1044.
18 T. Xu, P. Molnar, C. Gregory, M. Das, T. Boland and J. J. Hickman, *Biomaterials*, 2009, **30**, 4377–4383.
19 C. Zhong, J. Wu, C. Reinhart-King and C. Chu, *Acta Biomater.*, 2010, **6**, 3908–3918.
20 G. Sun, X. Zhang, Y.-I. Shen, R. Sebastian, L. E. Dickinson, K. Fox-Talbot, M. Reinblatt, C. Steenbergen, J. W. Harmon and S. Gerecht, *Proc. Natl. Acad. Sci. U. S. A.*, 2011, **108**, 20976–20981.
21 Y.-C. Chen, R.-Z. Lin, H. Qi, Y. Yang, H. Bae, J. M. Melero-Martin and A. Khademhosseini, *Adv. Funct. Mater.*, 2012, **22**, 2027–2039.
22 J. Wu, X. Wang, J. K. Keum, H. Zhou, M. Gelfer, C. A. Avila-Orta, H. Pan, W. Chen, S. M. Chiao and B. S. Hsiao, *J. Biomed. Mater. Res., Part A*, 2007, **80**, 800–812.
23 S. Gerecht, J. A. Burdick, L. S. Ferreira, S. A. Townsend, R. Langer and G. Vunjak-Novakovic, *Proc. Natl. Acad. Sci. U. S. A.*, 2007, **104**, 11298–11303.
24 K. Obara, M. Ishihara, T. Ishizuka, M. Fujita, Y. Ozeki, T. Maehara, Y. Saito, H. Yura, T. Matsui and H. Hattori, *Biomaterials*, 2003, **24**, 3437–3444.
25 J. A. Rowley, G. Madlambayan and D. J. Mooney, *Biomaterials*, 1999, **20**, 45–53.
26 A. Gaowa, T. Horibe, M. Kohno, K. Sato, H. Harada, M. Hiraoka, Y. Tabata and K. Kawakami, *J. Controlled Release*, 2014, **176**, 1–7.

27 S. A. Oh, H. Y. Lee, J. H. Lee, T. H. Kim, J. H. Jang, H. W. Kim and I. Wall, *Tissue Eng., Part A*, 2012, **18**, 1087–1100.
28 C. B. Hutson, J. W. Nichol, H. Aubin, H. Bae, S. Yamanlar, S. Al-Haque, S. T. Koshy and A. Khademhosseini, *Tissue Eng., Part A*, 2011, **17**, 1713–1723.
29 S.-M. Lien, L.-Y. Ko and T.-J. Huang, *Acta Biomater.*, 2009, **5**, 670–679.
30 Y.-H. Lin, H.-F. Liang, C.-K. Chung, M.-C. Chen and H.-W. Sung, *Biomaterials*, 2005, **26**, 2105–2113.
31 A. Bigi, G. Cojazzi, S. Panzavolta, N. Roveri and K. Rubini, *Biomaterials*, 2002, **23**, 4827–4832.
32 J. L. Ifkovits and J. A. Burdick, *Tissue Eng.*, 2007, **13**, 2369–2385.
33 R. M. K. Ramanan, P. Chellamuthu, L. Tang and K. T. Nguyen, *Biotechnol. Prog.*, 2006, **22**, 118–125.
34 N. Wang, X. S. Wu and J. K. Li, *Pharm. Res.*, 1999, **16**, 1430–1435.
35 J. D. Kretlow, L. Klouda and A. G. Mikos, *Adv. Drug Delivery Rev.*, 2007, **59**, 263–273.
36 X.-Z. Zhang, P. Jo Lewis and C.-C. Chu, *Biomaterials*, 2005, **26**, 3299–3309.
37 J. Wu, D. Wu, M. A. Mutschler and C. C. Chu, *Adv. Funct. Mater.*, 2012, **22**, 3815–3823.
38 L. A. Reis, L. L. Y. Chiu, Y. Liang, K. Hyunh, A. Momen and M. Radisic, *Acta Biomater.*, 2012, **8**, 1022–1036.
39 A. S. Hoffman, *Adv. Drug Delivery Rev.*, 2012, **64**(supplement), 18–23.
40 J. Wu, M. A. Mutschler and C.-C. Chu, *J. Mater. Sci.: Mater. Med.*, 2011, **22**, 469–479.
41 J. A. Benton, C. A. DeForest, V. Vivekanandan and K. S. Anseth, *Tissue Eng., Part A*, 2009, **15**, 3221–3230.
42 H. Shin, B. D. Olsen and A. Khademhosseini, *Biomaterials*, 2012, **33**, 3143–3152.
43 X. Zhao, Q. Lang, L. Yildirimer, Z. Y. Lin, W. G. Cui, N. Annabi, K. W. Ng, M. R. Dokmeci, A. M. Ghaemmaghami and A. Khademhosseini, *Adv. Healthcare Mater.*, 2015, DOI: 10.1002/adhm.201500005.

